Journal of Molecular Structure 1166 (2018) 79–90

Contents lists available at ScienceDirect

Journal of Molecular Structure

journal homepage: http://www.elsevier.com/locate/molstruc

Synthesis, characterization, molecular modeling, antioxidant and microbial properties of some Titanium(IV) complexes of schiff bases

Mohammad Nasir Uddin [a, *], Sonia Khandaker [a], Moniruzzaman [e], Md. Shaharier Amin [a], Wahhida Shumi [b], Md. Atiar Rahman [c], Sheikh Mahbubur Rahman [d]

[a] Department of Chemistry, University of Chittagong, Chittagong, 4331, Bangladesh
[b] Department of Microbiology, University of Chittagong, Chittagong, 4331, Bangladesh
[c] Department of Biochemistry & Molecular Biology, University of Chittagong, Chittagong, 4331, Bangladesh
[d] UL Laboratories, Dhaka, Bangladesh
[e] Department of Applied Chemistry and Biochemical Engineering, Shizuoka University, 3-5-1, Johoku, Hamamatsu, 432-8011, Japan

ARTICLE INFO

Article history:
Available online 6 April 2018

Keywords:
Schiff bases
Titanium(IV) complexes
Aroylhydrazine
Nicotinic acid hydrazide
Dibasic tridentate ligands
Computational study
Octahedral geometry
Anti-microbial and antioxidant properties

ABSTRACT

The titanium(IV) complexes of Schiff bases derived from aroylhydrazine e.g. benzoylhydrazine, salicyloylhydrazine, nicotinic acid hydrazide with aldehyde or ketone are reported and characterized based on UV–vis spectroscopy, (Infra-red) IR spectra, ^{1}H NMR spectra, mass spectra, magnetic susceptibility and molar conductance measurements. Complexes are found to possess 1:2 (metal:ligand) stoichiometry. The prepared ligands were act as dibasic tridentate ligands. On the basis of experimental evidences octahedral geometry has been proposed for prepared complexes. Geometry was confirmed by the optimized structure obtained from computational study. The synthesized ligands, in comparison to their titanium(IV) complexes, were also screened for their microbial and antioxidant properties.

1. Introduction

Schiff base ligands are considered as “privileged ligands” [1] because they are easily prepared by condensation between aldehydes and primary amines. The chemistry of transition metal complexes with Schiff bases has played an important role in the development of coordination chemistry as a whole. The field of Schiff base complexes is fast developing because of the wide variety of possible structures for the ligands, depending on the aldehyde and amines used. Many Schiff bases and their complexes have been widely studied because of their industrial and biological applications [2,3]. Hydrazones are the condensation products of hydrazine derivatives with carbonyl compounds, they contain an acyclic group >C═N–N<. It is long since hydrazones and their derivatives, due to their high complexing ability, have attracted the attention of scientists. Depending on various factors (the nature of the hydrazone and the metal atom, reaction conditions, the ratio of reactants etc.) hydrazones form either mono- or polynuclear coordination compounds with metal atoms [4]. Aroyl hydrazones and their metal derivatives often possess biological activity and can inhibit enzymatic reactions in the cell [5–7]. The remarkable biological activity of acid hydrazides, R–CO–NH–NH_2, a class of Schiff bases, their corresponding aroylhydrazones, R–CO–NH–N═CH-R and their dependence of their mode of chelation with transition metal ion present in the living system have been of significant interest. Isonicotinic acid hydrazide is a drug of proven therapeutic importance and is used bacterial ailments e.g. tuberculosis [8]. Diketones have been widely used as intermediates in the preparation of large number of biologically important heterocyclic compounds and as precursors of potential anti-diabetic drugs [9]. Metal complexes of S–, N–, and O-chelating ligands have attracted considerable attention because of their interesting physico-chemical properties, pronounced biological activities and their use as models for metalloenzyme active sites [10,11]. In this investigation, titanium(IV) complexes were synthesized from some new Schiff base ligands. They are characterized in terms of conventional techniques. Geometry of the ligands and complexes was optimized by computational chemistry study. Selected ligands and complexes were tested against the growth of bacteria and fungi. Also their antioxidant property was to evaluate.

* Corresponding author.
E-mail address: nasircu72@gmail.com (M.N. Uddin).

https://doi.org/10.1016/j.molstruc.2018.04.025
0022-2860/

2. Experimental

2.1. Instrumentation and apparatus

Electronic weighing balance, Microwave oven, Magnetic stirrer, Reflux condenser, Round bottom flasks, Beakers, Pipettes, Funnels, Water bath, Burners, Test tubes, Desiccator, Melting point apparatus, UV–Vis spectrophotometer, IR spectrometer, ^{1}H NMR Spectrometer, Mass Spectrometer, pH Meter, NMR spectrometer, Autoclave, Conical flask (250 mL), Test tubes, Micropipettes, Horizontal Laminar Flow Unit, Incubator, Micro tips etc.

2.2. Chemicals and solvents

Methanol, Ethanol, Nicotinic Acid Hydrazide, Ethyl Acetoacetate, Benzoyl Acetone, 2-Hydroxy-1-Naphthaldehyde, Dimethyl Sulfoxide, Dimethyl Formamide, Acetone, Chloroform, Diethyl ether, Titanium tetrachloride, Beef Extract, Peptone, 95% Ethanol, 70% Ethanol, Sterile Water, Potato, Dextrose, Agar, Distilled Water, Folin Ciocalteu Reagent (FCR), Na_2CO_3 (20% solution), Standard gallic acid, DPPH solution (2,2-diphenyl-1-picrylhydrazyl), Ascorbic acid etc.

2.2.1. Benzoyl hydrazine ($C_6H_5CONHNH_2$)

This compound was prepared (12) by refluxing an equimolar mixture of ethylbenzoate and hydrazine hydrate for 21 h. The product thus obtained was recrystallized twice from ethanol. Melting point 112°.

2.2.2. Salicyloylhydrazine (2-OH–C_6H_4CO–$NHNH_2$)

An equimolar mixture of ethylsalicylate and hydrazine hydrate was refluxed for 5 h where after the white solid mass obtained was recrystallized twice from hot water (12). Melting point 146°.

2.2.3. Synthesis of ligands

The Schiff Base ligands were synthesized by the following general procedure. The aliphatic or aromatic amine compound was dissolved in absolute methanol in a round bottom flask with constant stirring and heating. Then ketone or aldehyde was added drop wise. The mixture was heated under reflux for 2 h. The volume was allowed to reduce placing the reaction mixture in a water bath. After about 1 h heating the reaction mixture was allowed to cool at room temperature for 20 min. The solid precipitated was filtered off, and washed several times using absolute methanol. Then the solid precipitate dried over silica gel.

2.2.4. Synthesis of complexes

The ligand (10 mmol) was dissolved in absolute ethanol and 10 mmol $TiCl_4$ was added drop wise in it. Then the reaction mixture was refluxed for 3 h and allowed to cool at room temperature. Colour change was occurred for each complex. Then the metal complexes were separated by filtration and washed thoroughly with ethanol and dried in vacuo over silica gel and $CaCl_2$.

2.3. Computational study

The ligands and complexes were designed depending on quantum mechanical (QM) calculation. QM methods allow us to calculate different types of energies precisely and interpret various types of complicated interaction between ligands and metal in the formation of complexes [13]. In the present work, Density functional theory with Becke's, exchange functional combining Lee, Yang and Paee's correlation functional [14] in Gaussian 09 program package for the ligands and complexes [15]. Pople's 6-31G (d,p) basis set has been employed to optimize the ligands and complexes to elucidate their thermodynamic properties such as; thermal energy, enthalpy, Gibb's free energy, entropy, dipole moment and their electronic properties e.g. frontier molecular orbital features (HOMO, LUMO, HOMO-LUMO gap), hardness and softness [16].

Hardness and softness of all ligands and complexes were also calculated from the energies of frontier HOMOs and LUMOs considering Parr and Pearson interpretation [17] of hamess in DFT and Koopmans theorem [16] on the correlation of ionization potential (IP) and electron affinities (EA) with HOMO and LUMO energy. The following equations are used to calculate the Hardness (η) and Softness (S);

$$\eta = [\varepsilon\text{LUMO-}\varepsilon\text{HOMO}]\ /2;\ S = 1/\ \eta$$

2.4. Microbial property

All measurements of antifungal and antibacterial activities have been carried out and the test tube cultures of the bacterial pathogens were collected from the Department of Microbiology, University of Chittagong, Bangladesh.

2.4.1. Anti-bacterial property

List of test organisms which used in present research are *Staphylococcus aureus, Bacillus cereus, Salmonella paratyphi* and *Candida albicans*. Standard Nutrient Broth media consisting peptone (5 g), beef extract (3 g), NaCl (0.5 g), distilled water (1000 mL) was used throughout the study. 0.2%, 0.5% and 0.8% solutions were prepared by dissolving 0.002 g, 0.005 g and 0.008 g solid samples in 1 mL DMSO respectively. Small amount of the collected microorganisms were transferred to the nutrient agar containing test tubes with the help of sterilized needles. The inoculated tubes were incubated for 24 h at 37 °C.

A number of test tubes were freshly cleaned and 10 mL of prepared nutrient broth were placed in every test tube. The test tubes were then capped with cotton and sterilized by autoclaving at 15-lbs. pressure/sq. inch at 121 °C for 20 min. Then 100 μL prepared test sample solutions were added to the sterilized nutrient broth containing test tubes by micropipette. Then the 100 μL incubated selected microorganisms (freshly cultured) were carefully inoculated to these test tubes by micropipette. After inoculation, test tubes were incubated at 37 °C. Then the absorbance of every incubated solution was recorded by UV-Spectrophotometer at 600 nm after 6 h–24 h.

2.4.2. Antifungal activities

The prepared ligands and complexes were tested in vitro against fungi by two methods. One was by liquid medium method against *Fusarium* and another was by disc diffusion technique against *Aspergillus niger*. 0.8% solutions were prepared by dissolving 0.008 g solid samples in 1 mL DMSO.

2.4.3. Culture media

PDA (Potato-Dextrose-Agar) medium was used as culture media and it was prepared by the composition of Potato (200 g), Dextrose (20 g), Agar (15 g), Distilled Water (1000 mL). To prepare PDA medium, potatoes were cut into pieces and weighed about 200 g and boiled in 1000 mL of distilled water for an hour, filtered and volume was made up to 1000 mL by adding more distilled water. Glucose and agar were then added and stirred. The pH of the medium was checked and recorded. The medium was then sterilized at 121 °C temperature and 15 lb pressure 25 min.

2.4.4. Liquid medium method

A number of conical flasks were freshly cleaned and 20 mL of prepared LPD media [18] was taken in every conical flask. The conical flasks were then capped with cotton and sterilized by autoclaving at 15-lbs. pressure/sq. inch at 121 °C for 20 min. Then 200 μL prepared sample solutions were added to the sterilized LPD media containing conical flasks by micropipette. Then selected microorganism was carefully added to these conical flasks by a loop. After adding the microorganism test tubes were incubated for 3 days. Same procedure was performed without adding microorganism and was recorded pH instant and after 3 days to observe the activity of the sample and the solvent. After 3 days all the organism containing solutions were filtered and separated the growing organism from the solutions. The filtered growing organism dried in oven at 60 °C. Then pH of the filtered solutions was taken by pH meter.

2.4.5. Cup plate technique

The prepared ligands and complexes were tested in vitro against fungi *Aspergillus niger* by cup plate technique also [19]. PDA was used as culture media. The culture media prepared without agar powder is called nutrient broth. Nutrient broth was inoculated with the fungal suspension with the help of an inoculating loop in an aseptic condition, mixed thoroughly and kept in shaker for 2 days in order to facilitate the case of homogeneous distribution at 37 °C. This type of liquid culture is called broth culture. Fresh culture of this type was always used throughout the sensitivity testing.

The test ligands and complexes were mixed with sterilized liquid media. The medium was poured into sterile petridishes in an aseptic condition on a leveled horizontal surface so as to give a uniform depth of approximately 4 mm. Then the medium had been allowed to cool to room temperature in order to solidify the medium. Sterilized cork borer was taken and the test fungus (*Aspergillus niger*) plate were cut by the borer. One colony with the help of sterilized needle was transferred into the prepared solid plate. After transferring, the plates were incubated at 27 °C for 2–3 days. The zone of growth or zone of inhibition was measured and recorded.

2.5. Antioxidant properties

Some prepared Schiff base ligands and complexes were tested for antioxidant property. This experiment was carried out at Department of Biochemistry and Molecular Biology, University of Chittagong. Total Phenolic Content Determination (TPC) and DPPH Free Radical Scavenging Activity experiments were done to evaluate the antioxidant property of ligands and complexes.

2.5.1. Determination of total phenolic content (TPC)

Total phenolic content of test samples were determined by a method established by with some modification using FCR (Folin Ciocalteu Reagent) [20]. The test samples were oxidized with FCR and the reaction was neutralized with sodium carbonate. The absorbance was measured at 760 nm. The phenolic content was expressed as Gallic acid equivalents using the following linear equation based on the calibration curve. The result was expressed in micrograms equivalent gallic acid by grams of the powder dry mass of the test samples (μg GAE/g).

At first 20 μL sample or 20 μL standard solution was taken in screw cap tube and then added 1.58 mL distilled water to the tube. After that 100 μL FC reagent was added and incubated at room temperature for 1–8 min. Then 300 μL Na_2CO_3 solutions was added into the tube and incubated at room temperature for 2 h. Finally optical density (OD) of the solution was measured at 760 nm (Note: Used distilled water as blank).

2.5.2. DPPH free radical scavenging activity

A certain amount of sample was dissolved in DMSO to prepare the stock solution. Standard solution: 1000 mg of ascorbic acid was dissolved in 10 mL of solvent (by which extract prepared) to prepare 1 μg\mL. 0.4 mM DPPH solution: 0.158 g of DPPH (MW 394.32) was dissolved in 100 mL of methanol and the solution was kept in conical flask. It was protected from the light by covering the flask with aluminium foil.

Procedure [21]: A 2.5 mL of different concentrations of ascorbic acid (30, 60, 120, 240 and 480 μg mL^{-1}) were taken in triplicate numbers of test tubes. Then 2.5 mL of different concentrations of test sample (30, 60, 120, 240 and 480 μg mL^{-1}) were taken in triplicate numbers of test tubes. A 2.5 mL of distilled water was taken in duplicate pair of test tubes for control in case of standard, and 2.5 mL of DMSO was taken in duplicate pair of test tubes for control in case of test samples. **1.5** mL of 0.4 mM DPPH solution was mixed in all of the above test tubes. The test tubes were kept in dark for 30 min at room temperature for complete reaction. The degree of DPPH decolourisation to yellow indicates the scavenging efficiency of the extracts. Then the absorbance of the solution was measured at 517 nm using a spectrophotometer against blank (methanol). Lower absorbance of the reaction mixture indicated higher free radical-scavenging activity.

DPPH radical scavenging activity was calculated according to the following equation:

$$\text{DPPH radical scavenging } (\%) = \left[1 - \left(\frac{As}{Ac}\right) x\ 100\right]$$

here, Ac = absorbance of control, As = absorbance of sample solution.

Then % of inhibition was plotted against respective concentrations used and from graph IC_{50} was calculated.

3. Results and discussion

3.1. Physical properties of prepared ligands and complexes

All the prepared ligands and complexes were coloured compound with high melting point >200 °C.The melting point of most of the ligands was less than the prepared complexes. Both ligands and complexes were quite stable at room temperature and can be stored for a long time. They were insoluble in water but completely soluble in both DMSO and DMF. The physical properties of prepared Schiff base ligands and complexes are given in table-1.

3.2. Infrared spectra

The bands obtained in the region 3160-3270 cm^{-1} for the aroylhydrazones bases are attributed to *ν*-N–H. Pickard and Polly [11] reported the *ν*N-H frequencies near 3200 cm^{-1} for a number of ketimines. Association of the N–H group with ketonic group gives absorption in the range 3240–3320 cm^{-1}. The β-diketone hydrazone ligands seem to exist in the keto form and do not show enolic OH bands. In o-hydroxycarbonyl-hydrazones there is no band above 3270 cm^{-1} due to the free OH group thus showing it to be hydrogen bonded with the azomethine nitrogen [12]. In the infrared spectra of the free ligands, generally two bands are observed in the region 3040-3380 cm^{-1}. One of these two bands above 3000 cm^{-1} is due to the hydrogen OH group and the other being due to the free of hydrogen bonded N–H [4]. The broad band around 3200 cm^{-1} might be a mixture of *ν*N-H and H-bonded phenolic/enolic OH stretches. The bands observed between 1640 cm^{-1} and 1675 cm^{-1} for the free ligands are due to νC = O and that obtained at 1600-1632 cm^{-1} are due to *ν*C = N of the

azomethine group [6,8]. The bands obtained at 1530-1580 cm^{-1} are due to the $\nu C=C$ aromatic [6,12].

In the infrared spectra of the TiL_2 complexes, the absence of the νO-H frequency indicates deprotonation of both are replaceable hydrogen atoms and the dibasic character of the benzoylhydrazone Schiff bases. A representative IR spectrum is shown in Fig. 1. The spectra of the complexes show no characteristic bands for the νN-H and $\nu C=O$ in agreement with the ligands being coordinated in the enolic form. This mode of coordination is further supported in each case by the appearances of the $\nu C=N$ band at about 1600 cm^{-1}. The $\nu C=N$ present in the free ligand show a downward shift of 10–35 cm^{-1} indicating the involvement of the nitrogen of the azomethine group in coordination [11]. The bands appearing around 1600 cm^{-1} seems to originate from the stretching mode of the conjugate >C═N–N═C< grouping [7,12] suggesting the enolization of the ligand in presence of Ti^{4+} and the participation of the enolic oxygen in coordination. Also, as stated above, the disappearance of all bands above 3000 cm^{-1} confirms the participation of the phenolic and enolic oxygen in coordination on deprotonation. The bands appearing at 1250-1372 cm^{-1} have been assigned as due to νC–O (phenolic/enolic). The formation of the TiL_2 compounds is also indicated by the appearance of the νN-N at a higher frequency as compared to that in the free ligand [11,12].

The bands characteristic of $\nu Ti=O$ were absent in the TiL_2 complexes thus indicating the presence of the non-oxotitanium (IV) in these present metal chelates. Based on the previous results [11,12], the bands appearing for the present systems at 530-600 cm^{-1} and 400-470 cm^{-1} have been assigned tentatively to Ti–N and Ti–O stretching frequencies respectively. These νTi-N and νTi-O band regions seem reasonable on the basis of some other M-N and M-O band regions observed for some other metal complexes of related systems [4–7]. These νTi-N and νTi-O assignments (Table 4) are less definitive and tentative. The presence of a smaller number of bands in this region was an advantage for attempts of the present assignments. Some infrared spectral data along with their tentative assignments for the free ligands and for the TiL_2 complexes of these ligands are given in Table 2.

3.3. Electronic spectra

The electronic spectra of the some prepared TiL_2 complexes were run in DMF and some were in DMSO solutions recorded in the 250–500 nm region (Table 2). The electronic spectral data of the free ligands and the TiL_2 complexes are given in Table 5. The spectra of the Schiff base $L\underline{H}_2$ exhibit three main peaks at around 270, 320 and 370 nm. The first and second peaks around 270, 320 nm were attributed to aryl π-π*and iminoπ-π* (–C═N) transitions respectively [22]. The first band of the other complexes of the Schiff base $L\underline{H}_2$ was not significantly affected by chelation. The second band was shifted to a shorter wavelength by chelation. The third in the spectra of $L\underline{H}_2$ (~370 nm) was assigned to n-π* transitions [23]. This band was shifted to a longer wavelength along with an increase in its intensity. This shift may be attributed to the donation of the lone pairs of the nitrogen atoms of the Schiff base $L\underline{H}_2$ to the metal ion (N-M). Similar observation was observation was obtained for the prepared complexes. The electronic spectra of the complexes showed bands similar to those observed for the free ligands. There is no evidence of any d-d transition, for the TiL_2 complexes, over the visible region. The bands in the longer wavelength region may be attributed to be LMCT transition. The complexes are coloured only through these intense charge transfer absorptions tailing in from the ultraviolet. Being a d^0 system, the present complex system should not show any d-d but C.T transitions. The other bands (Table 2) observed are all intense and may be assigned to the π–>π* (benzoid and azomethine) and n–>π* (azomethine) transitions as well as to the C.T. The electronic spectral behaviour of the complexes suggests that the complexes are genuine d^0-Ti(IV) species rather than any Ti(III). Representative electronic spectra of a ligand and its complex have been shown in Fig. 2.

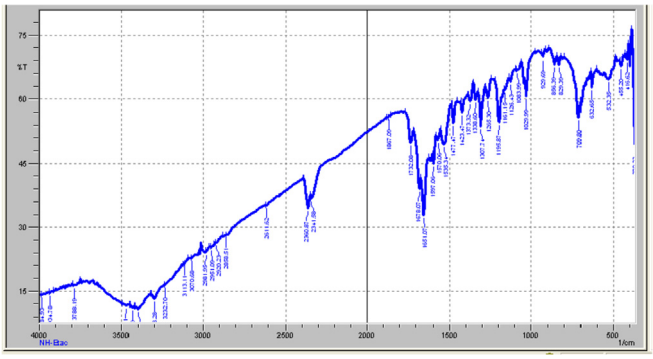

Fig. 1. IR spectrum of $Ti(NH.Bzac)_2$.

3.4. Conductance and magnetic measurements

Magnetic measurements were performed at room temperature.

Table-1
The physical properties of prepared Schiff base ligands and complexes.

Serial No	Ligands/complexes	Molecular Formula	Melting point	Solubility	Colour	Yield %
1	Etac-B$H\underline{H}_2$	$C_{13}H_{16}N_2O_3$	245 °C	DMF	Pink	70
2	Bzac-B$H\underline{H}_2$	$C_{17}H_{16}N_2O_2$	133 °C	DMF	White	70
3	Etac-Sal$H\underline{H}_2$	$C_{13}H_{16}N_2O_4$	134 °C	DMF	Cream	90
4	Bzac-Sal$H\underline{H}_2$	$C_{17}H_{16}N_2O_3$	206 °C	DMF	Yellow	75
5	Etac-NH $\underline{H}_2$	$C_{12}H_{15}N_3O_3$	(193–197)°C	DMSO	Off White	65
6	Bzac-N$H\underline{H}_2$	$C_{16}H_{15}N_3O_2$	(130–135)°C	DMSO	Yellow	78
7	HNP–B$H\underline{H}_2$	$C_{18}H_{14}N_2O_2$	>200 °C	DMSO	Chocolate	75
8	HNP-Sal$H\underline{H}_2$		>200 °C	DMSO	Chocolate	80
9	HNP–N$H\underline{H}_2$	$C_{17}H_{13}N_3O_2$	>200 °C	DMSO	Light Chocolate	74
1	Ti (Etac-BH)$_2$	$TiC_{26}H_{28}N_4O_6$	>250 °C	DMF	Cream	60
2	Ti (Bzac-BH)$_2$	$TiC_{34}H_{28}N_4O_4$	250 °C	DMF	Black	70
3	Ti (Etac-SalH)$_2$	$TiC_{26}H_{26}N_4O_6$	>250 °C	DMF	Orange	75
4	Ti (Bzac-SalH)$_2$	$TiC_{34}H_{28}O_6N_4$	>260 °C	DMF	Black	65
5	Ti (Etac-NH)$_2$	$TiC_{24}H_{26}N_6O_6$	>200 °C	DMSO	Brown	60
6	Ti(Bzac-NH)$_2$	$TiC_{32}H_{26}N_6O_4$	(192–196)°C	DMSO	White	75
7	Ti(HNP–BH)$_2$	$TiC_{36}H_{24}N_4O_4$	>200 °C	DMSO	Wine red	81
8	Ti (HNP-SalH)$_2$		>200 °C	DMSO	Chocolate	84
9	Ti(HNP–NH)$_2$	$TiC_{34}H_{22}N_6O_4$	>200 °C	DMSO	Chocolate	80

Table-2
Some characteristic infrared frequencies (cm^{-1}) and electronic spectral data (nm) for the Schiff base ligands.

Ligands/complexes	Infrared frequencies (cm^{-1})							Electronic spectra (nm)
	*v*C=O	*v*C=N	*v*C=C	*v*C–O	*v*N–N	*v*Ti–N	*v*Ti–O	
Etac-BH$\underline{H}_2$	1670 m	1632 s	1580 s	1285 vs	925 m			300flsh, 270
Ti(Etac-BH)$_2$		1595 s	1520 ms	1290 m	1020 m	580 w	430 w	350, 341, 299, 254
Bzac-BH$\underline{H}_2$	1660 s	1600 m	1550 ms	1280 s	920vs			430flsh, 342, 330flsh, 271
Ti(Bzac-BH)$_2$		1590 vs	1545 s	1290 s	950 m	595 s	430 m	421flsh, 355sh, 299, 287flsh
Etac-SalH$\underline{H}_2$	1720 vs	1625 s	1550 s	1275 s	905 s			365flsh, 301sh, 273
Ti(Etac-SalH)$_2$		1595 s	1500 sbr	1250 vs	1030 s	530 w 600 ms	460 m	370flsh, 308sh, 277
Bzac-SalH$\underline{H}_2$	1635 m	1600 m	1530 ms	1300 ms	870 vs			420, 356sh, 321, 302flsh, 272
Ti(Bzac-SalH)$_2$		1590 s	1520 ms	1372 m	1020 m	670 m 580 w	470 ms 400 w	419, 359, 301, 275flsh
Etac-NH$\underline{H}_2$	1678 w	1651 s 1597 w	1535 m 1570 w	1265 m 1307 s	929 m			308sh, 267, 258, 238
Ti(Etac-NH)$_2$		1604 w	1469 s	1261 w 1280 s	1014 m 1040 w	594 w 621 m	474 w	260, 242, 232
Bzac-NH$\underline{H}_2$	1685 vs	1593 s	1577 ms	1292 w	929 s 879 s			589, 335, 233, 209
Ti(Bzac-NH)$_2$		1593.20 s	1531 ms	1265 vs 1396 m	1010 w	652 w 671 ms	459 m	498, 340, 271
HNP–BH$\underline{H}_2$	1604 m	1573 s	1465 s	1288 s	914 m 860 m			376, 363, 326, 313, 259
Ti(HNP–BH)$_2$		1597 vs	1408 s	1288 ms 1338 s	914 m 1037 w	582 s 648 ms	420 m	361, 353, 327, 311, 264
HNP-SalH$\underline{H}_2$	1633 vs	1507 s	1416 ms	1268 s	856 m			346, 307, 300, 244
Ti(HNP-SalH)$_2$		1501 ms	1407 s	1259 s	958 ms	625 w	462 m	386, 353, 307, 234
HNP–NH$\underline{H}_2$	1693 vs	1577 s	1516 ms	1288 vs	910 m 860 m			364, 327, 314, 259
Ti(HNP–NH)$_2$		1601 ms	1577 s	1280 s 1319 vs	1030 m 952 ms	621 w 655 m	420 m 474 w	410, 330, 262, 232

The measured magnetic susceptibility values (Table 3) suggest diamagnetic behaviour supporting $3d^0$ electronic configuration consistent with the 4 + oxidation state of central metal ion in complexes. The very low molar conductance values obtained in the 2.81–16.50 Ω^{-1} cm^2 mol^{-1} range [24], in DMF and DMSO solutions, for the complexes show them to be non-electrolyte in nature. Thus it is evident that there were no inorganic anions present outside the coordination sphere. The very low molar conductance values in DMF solutions also support the neutralization of the 4 + oxidation state of the central titanium ion by the two coordinated dinegatively charged tridentate ligands in these complex systems. Table 6 also shows the molar conductance values of the complexes.

3.5. ^1H NMR spectra

The ^1H NMR spectra of the compounds were obtained in DMSO at room temperature using TMS as an internal standard. The ^1H NMR data and assignments of the compounds are presented in Table 3. The free LH_2 ligands exhibit a peak between 11.116 and 13.19 ppm, which is due to hydrogen-bonded phenolic protons. This peak is due to hydrogen bonded phenolic protons and the integration is generally less than 2.0 due to this intramolecular hydrogen bonding. The chemical shift observed for the OH protons in the ligands was not observed in any of the complexes. The disappearance of the singlet signals for the OH proton in the ^1H NMR spectra of the complexes indicating the enolic oxygen atoms are coordinated to the central metal atom via deprotonation. The same result was confirmed by the IR spectra. The presence of a sharp singlet for the CH=C proton at 5.7 ppm and 6.047 ppm respectively clearly showed a up field shift compared to the free ligand and indicated that the magnetic environment is equivalent for all such protons. The ^1H NMR spectra of all the complexes showed a downfield shift in the frequency of azomethine protons confirming coordination of the metal ion [25]. This down field shift observation may be assigned to the deshielding of protons as a result of the reduction of electron density after coordination [26]. The multiplets of aromatic protons appeared within the range 7.4–8.2 ppm and they were not affected by chelation. The azomethine ($H_3C–C=N$) resonance signal is appeared at 2.27 ppm for Ti(Etac-NH)$_2$ [11,12]. This downfield chemical shift observation showed the coordination of the azomethine nitrogen to central atom [27]. On the basis of the physical and spectral data of the Schiff bases and the complexes discussed above, it is assume that the metal ions are bonded to the Schiff bases via the phenolic oxygen and the iminonitrogen. Fig. 3 shows the NMR spectrum of Ti(Etac.NH)$_2$.

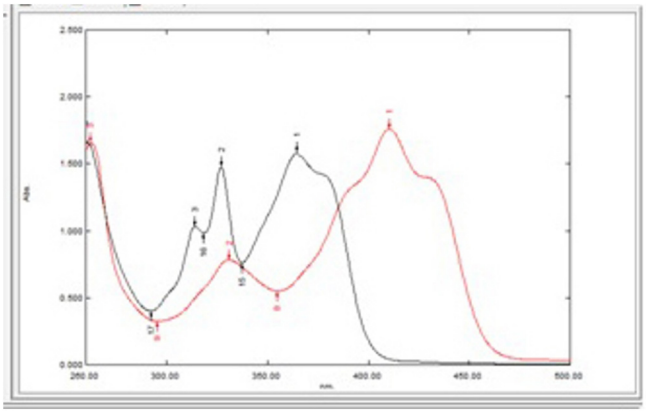

Fig. 2. Electronic spectra of NH·HNP, Red-Complex and Blue-Ligand.

3.6. Mass spectra

The mass spectra of Etac.NH$\underline{H}_2$, Ti(Etac.NH)$_2$, BH·HNP$\underline{H}_2$ and

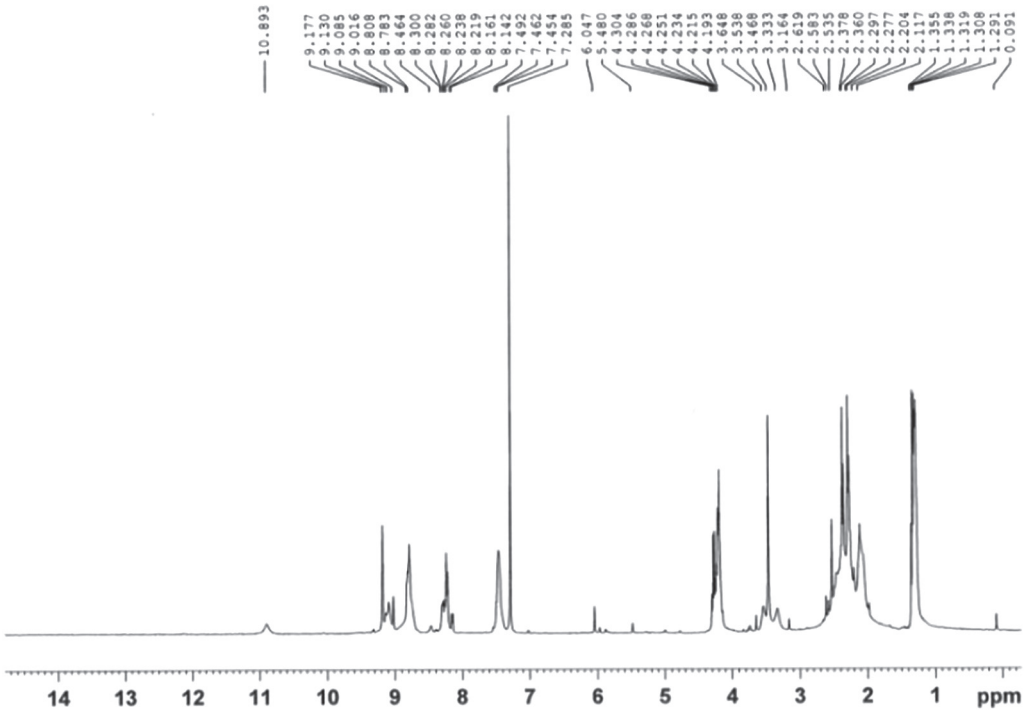

Fig. 3. NMR spectrum of Ti(Etac.NH)$_2$.

Table-3
^{1}H NMR spectral data, Magnetic and conductance data of the selected ligands and titanium complexes.

Complexes	^{1}H NMR (DMSO)						Conductance		μ (B.M)
	−CH_3	−CH_2−	−CH=	=CH−(Ar)	−OH	Ar−H	Solvent	Λ_M Ohm^{-1} cm^2 mole^{-1}	
Ti(Etac-BH)$_2$							DMF	5.0	Dia
Ti(Bzac-BH)$_2$							DMF	2.5	Dia
Ti(Etac-SalH)$_2$							DMF	4.8	Dia
Ti(Bzac-alH)$_2$							DMF	8.5	Dia
Etac.NH$\underline{H}_2$	2.079 2.509	3.71	5.7	–	11.116	7.7–9.2			
Ti(Etac-NH)$_2$	1.29 2.27	3.451	6.047	–	–	7.46–9.1	DMSO	7.7	Dia
BH·NH$\underline{H}_2$	–	–	–	7.175	13.19	7.5–7.9			
Ti(Bzac-NH)$_2$	–	–	–	6.4	–	7.02–8.210	DMSO	10.4	Dia
Ti(HNP−NH)$_2$							DMSO	6.4	Dia
Ti(HNP−BH)$_2$							DMSO	4.4	Dia

Ti(BH·HNP)$_2$ show molecular ion peak at $m/z = 250.6$, $m/z = 542.4$, $m/z = 289.2$ and $m/z = 622.6$ respectively which correspond to the molecular weight of the respective compound, corresponds to [M+1] supports to the structure of the complexes and confirms the ML type stoichiometry of the metal chelates. The series of peaks, in the ranges of 109.1, 147.1, 162.2, 175.2, 204.2, 221.2 and 234.2 may be corresponding to various fragments of Etac.NH$\underline{H}_2$ and their intensity gives an idea of stability fragments. The mass Spectrum of Ti(Etac.NH)$_2$ shows the series of peaks at 260.1, 322.1, 350.1, 386.1, 422.2, 452.2, 486.3, 514.3 may correspond to various fragments and their intensity gives an idea of the stability of these fragments. Fig. 4 shows the mass spectrum of Ti(Etac.NH)$_2$ Fig. 5 shows mass fragmentation pattern of this comple. The series of peaks, in the ranges of 110.60, 161.2, 173.2, 198.2, 210.2, 262.3 and 274.3 may be corresponding to various fragments of BH·HNP$\underline{H}_2$ and their intensity gives an idea of stability fragments. An 'isotope' of any given element is an atom with the same number of protons but a different number of neutrons, resulting in a different overall mass. Almost all elements have a variety of naturally occurring isotopes. For isotopic abundance, some fragments were found in which one or two units were less or more than the calculated value.

3.7. Computational studies

The thermodynamic properties of the ligands and complexes are also computed at PBEPBE/SDD level of theory, and the results are summerizes in Table 4. The thermal energy, enthalpy, Gibb's free energy of ligand Etac-NH$\underline{H}_2$ is greater than the ligand BH−HNP$\underline{H}_2$ and the complex Ti(Etac-NH)$_2$ is greater than the complex Ti(B-H−HNP)$_2$. Dipole moment is another important parameter in the study of ligand and complex formation system, drug-receptor systems and plays a significant role for the formation of hydrogen bond in the biological system. With the increase of dipole moment there is an increase of polarity of the compound. As a result increase the tendency of hydrogen bond formation, and also show a better effect in nonbonding interaction with selected protein in biological

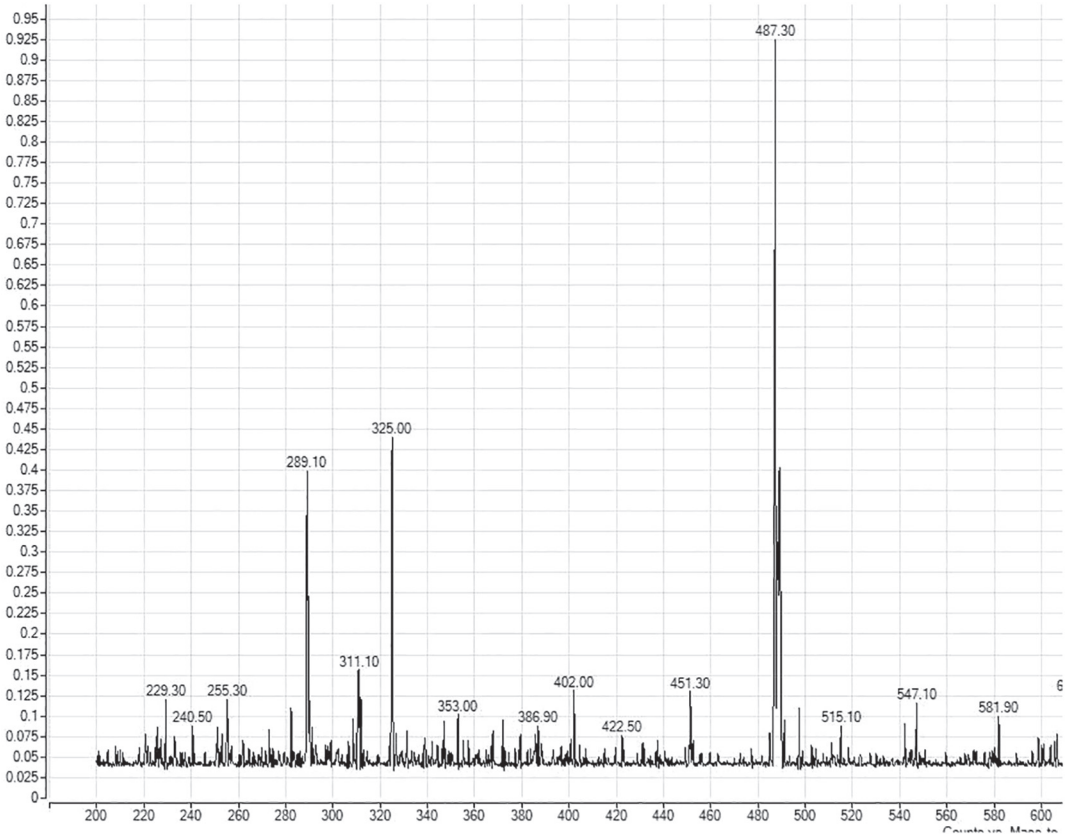

Fig. 4. Mass spectrum of $Ti(Etac\text{-}NH)_2$.

system [28]. It has been observed that there is an increase of dipole moment in ligand $BH\cdot HNPH_2$ as compare to ligand $Etac.HNPH_2$. On the other hand there is a significant increase of dipole moment in complex $Ti(Etac.NH)_2$ as compare to other complex $Ti(BH\cdot HNP)_2$. Optimized structure of two ligands and their respective complexes has been shown in Fig. 6.

3.7.1. Frontier molecular orbital

Frontier Molecular orbitals calculation is performed with the optimized structures of all ligands and coplmexes by using PBEPBE/SDD level of theory. Frontier orbitals energy values are important to determine chemical reactivity and the extent to which a drug interacts with a particular receptor which is defined as a highest occupied molecular orbital (HOMO) lowest unoccupied molecular orbital (LUMO) [29]. The energy gap between HOMO and LUMO predicts of a molecule's kinetic and chemical stability [30]. Larger the FO gap, higher the kinetic stability, as it is energetically unfavourable for an electron to have it elevated from a low energy HOMO to a relatively high-lying LUMO. The pictorial presentation of HOMO and LUMOs of some ligands and their complexes are shown in Fig. 7. Energy (eV) of HOMO, LUMO, Gap, hardness, and softness of all ligands are given in Table 5. Among the ligands and complexes it is found that the HOMO and LUMO energy gap for $Etac\text{-}NHH_2$ is the highest and for $Ti(BH{-}HNP)_2$ is the lowest. Chemical hardness and softness of a molecule also depend on HOMO-LUMO gap of a molecule. In this analysis, we found that ligand $BH\cdot HNPH_2$ has the lowest HOMO-LUMO gap and the highest softness, which may contribute to its higher chemical activity than other. A decreased HOMO-LUMO gap in ligands and complexes promotes softness which makes them relatively more polarizable and chemically more reactive compare to others [17].

3.8. Microbial properties

3.8.1. Antibacterial activities

Antibacterial activities were done by liquid medium method by measuring absorbance by spectrophotometer at 600 nm. Bacterial growth was evaluated after 6 h–24 h incubation in presence of ligands and complexes. The optical density of *Bacillus cereus*, *Staphylococcus aureus*, *Candida albicans* and *Salmonella paratyphi* were recorded for all ligands and complexes. Fig. 8 is the representative Presentation of bacterial activity of $Etac\text{-}NHH_2$.

$Etac\text{-}NHH_2$ ligand showed nearly the same activity as the control against *Bacillus cereus*, *Staphylococcus aureus* and *Salmonella paratyphi*. Maximum growth of bacteria was found at higher concentration against *Candida albicans* after both 6 h and 24 h incubation. Whereas its complex $Ti(Etac\text{-}NH)_2$ showed maximum enhancing capacity at 0.2% concentration and minimum at 0.8% concentration against the four test organisms.

In case of $Bzac\text{-}NHH_2$ ligand inducing capacity was increased with increasing concentration of sample against *Salmonella paratyphi*. Maximum enhancing capacity was found after 24 h incubation and minimum was found after 6 h incubation against the test organisms. Maximum growth for $Ti(Bazc\text{-}NH)_2$ was found at 0.5% and 0.8% concentration after both 6 h and 24 h incubation against *Salmonella paratyphi*. In case of *Candida albicans* and *Staphylococcus aureus* this complex showed higher enhancing capacity after 24 h incubation. But it showed higher inducing capacity at lower concentration against *Bacillus cereus*.

Ligand $NH\cdot HNPH_2$ showed nearly the same activity as the

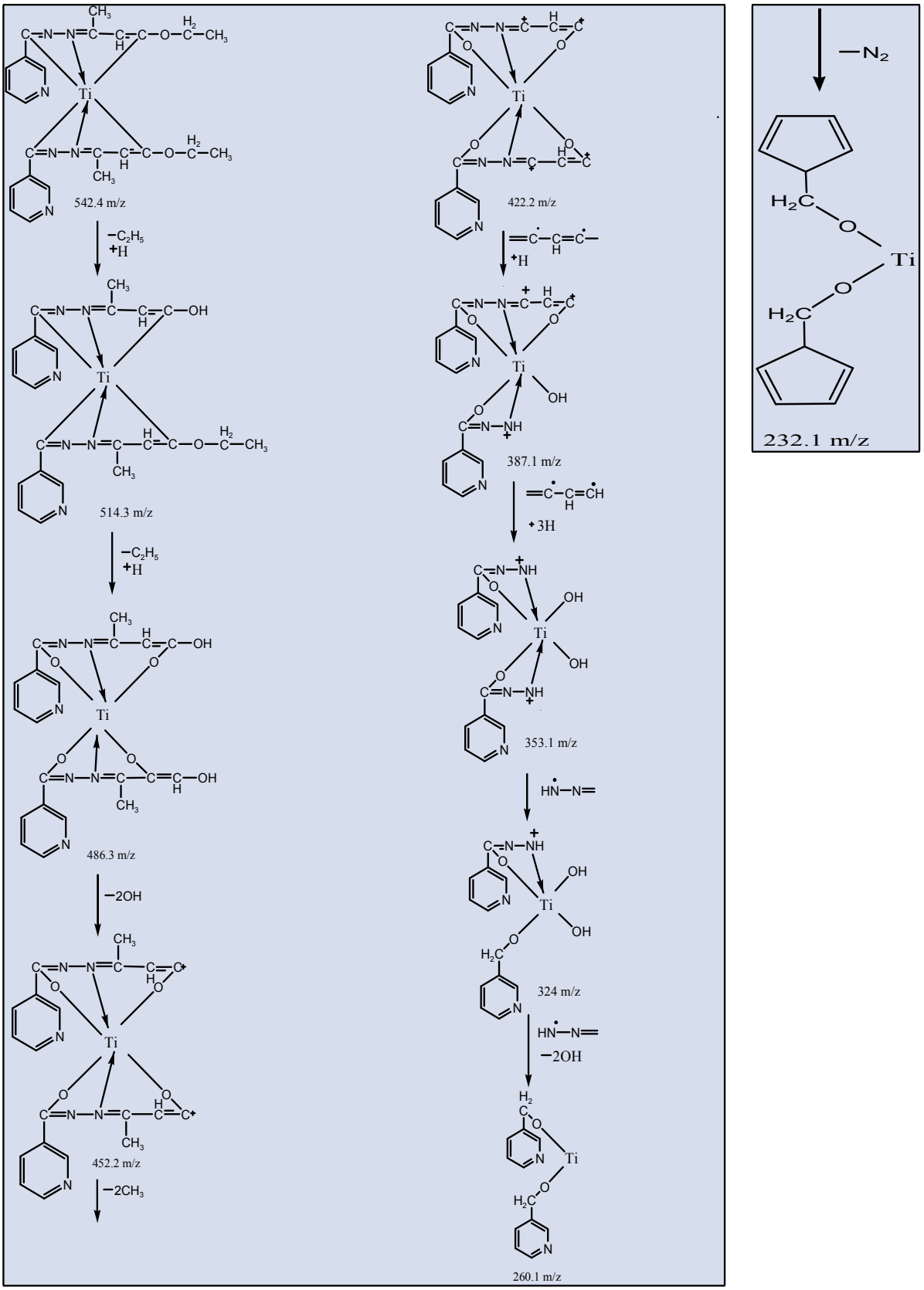

Fig. 5. Mass fragmentation pattern of $Ti(Etac.NH)_2$.

Table 4
The molecular formula, electronic energy, enthalpy, Gibbs free energy in kcal/mol, and dipole moment (Debye) of all ligands and complexes.

Name	Electronic energy	Enthalpy	Gibbs free energy	Dipole moment
Etac-BH$\underline{H}_2$	−835.2685	−835.2675	−835.3360	3.8391
Bzac-BH$\underline{H}_2$	−912.0153	−912.0144	−912.0822	2.2785
Etac-SalH$\underline{H}_2$	−910.0842	−910.0833	−910.1524	8.1133
Bzac-SalH$\underline{H}_2$	−986.8225	−986.8215	−986.8927	6.7737
Etac-NH$\underline{H}_2$	−851.2181	−851.2172	−851.2829	1.1971
Bzac-NH$\underline{H}_2$	−927.9593	−927.9583	−928.0285	3.2857
HNP−NH$\underline{H}_2$	−964.6676	−964.6666	−964.7315	4.3859
HNP−BH$\underline{H}_2$	−948.7227	−948.7218	−948.7860	2.1477
Ti(Etac-BH$\underline{H}_2$)	−2438.9840	−2438.9829	−2439.0090	3.0041
Ti(Bzac-BH$\underline{H}_2$)	−2667.2440	−2667.2431	−2667.3603	4.2559
Ti(Etac-SalH$\underline{H}_2$)	−2663.4989	−2663.4979	−2663.6085	3.4160
Ti(Bzac-SalH$\underline{H}_2$)	−2881.5217	−2881.5210	−2881.6313	6.2309
Ti(Etac-NH$\underline{H}_2$)	−2485.5568	−2485.5558	−2485.6663	3.2305
Ti(Bzac-NH$\underline{H}_2$)	−2709.6411	−2709.6400	−2709.7507	2.9807
Ti(HNP−NH$\underline{H}_2$)	−2816.8294	−2816.8283	−2816.9390	4.0075
Ti(HNP−BH$\underline{H}_2$)	−2770.2703	−2770.2692	−2770.375	3.5402

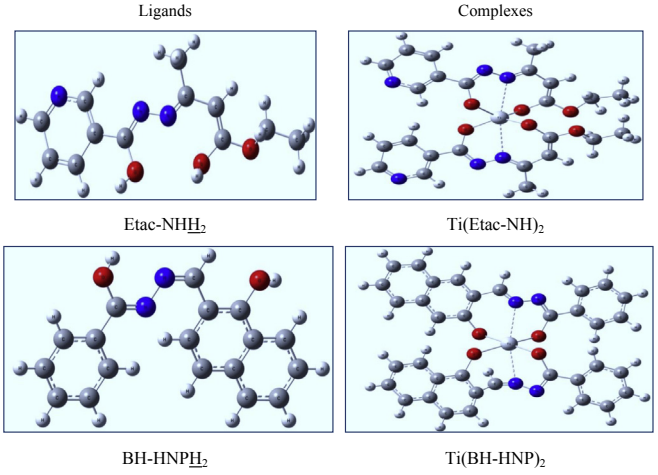

Fig. 6. Optimized structure of two ligands and their respective complexes.

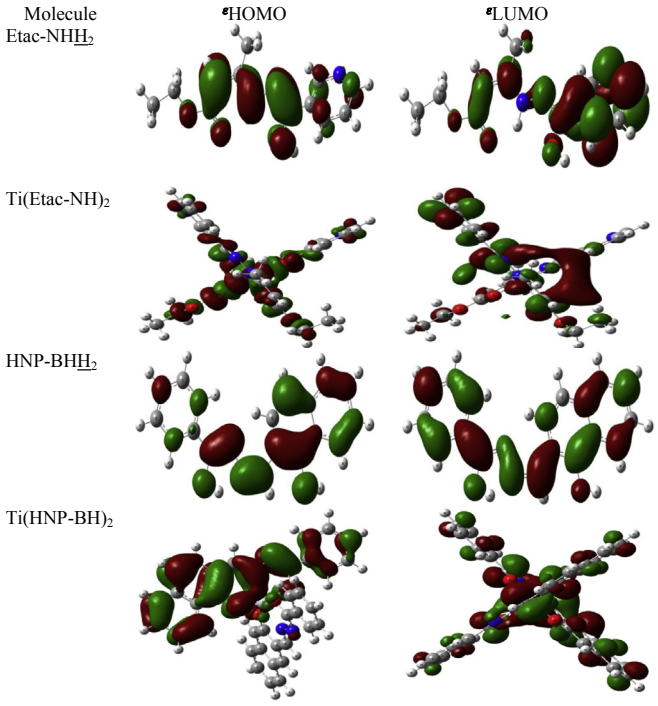

Fig. 7. The HOMO and LUMO of the ligands and complexes are showing below.

control after 24 h incubation against *Staphylococcus aureus* and *Candida albicans* and showed slightly inhibiting capacity against *Bacillus cereus* after 24 h incubation. Maximum inducing capacity was found after both 6 h and 24 h incubation at 0.5% concentration in case of *Salmonella paratyphi*. Its Ti(NH−HNP)$_2$ complex showed maximum enhancing capacity at 0.8% concentration after 24 h incubation and minimum was found in both 0.2% and 0.8% concentration against the test organisms.

BH·HNPH$_2$ ligand showed slightly inhibiting capacity after 6 h incubation but showed inducing activity after 24 h incubation against *Bacillus cereus*, *Candida albicans* and *Salmonella paratyphi*. In case of *Staphylococcus aureus* inducing capacity was increasing with increasing concentration of sample. Ti(BH.HNP)$_2$ complex induced the growth of test organism. It showed minimum enhancing capacity at 0.5% concentration with *Bacillus cereus* and *Staphylococcus aureus*, whereas maximum inducing capacity at 0.8% concentration with *Candida albicans* and *Salmonella paratyphi*.

It is seen that the growth of bacteria in sample solutions was higher than the growth of bacteria growth in control. That indicates that ligands and complexes were showing the inducing activity rather than the inhabiting activity against the test organisms.

3.8.2. Antifungal activities

3.8.2.1. Liquid medium method. The prepared ligands and complexes were tested by liquid media method by measuring pH of the

Table 5
Energy (eV) of HOMO, LUMO, Gap, hardness, and softness of all ligands.

Molecule	εHOMO	εLUMO	Gap	Hardness (η)	Softness(S)
Etac-BH$\underline{H}_2$	−6.2828	−1.0694	5.2134	2.6067	0.3836
Bzac-BH$\underline{H}_2$	−6.3960	−1.8397	4.5563	2.2782	0.4389
Etac-SalH$\underline{H}_2$	−5.3720	−1.2258	4.1462	2.0731	0.4824
Bzac-SalH$\underline{H}_2$	−5.5029	−2.0049	3.4980	1.7490	0.5717
Etac-NH$\underline{H}_2$	−6.4374	−1.5216	4.9158	2.4579	0.4068
Bzac-NH$\underline{H}_2$	−6.3759	−1.7415	4.6344	2.3172	0.4315
HNP−NH$\underline{H}_2$	−5.6597	−1.8095	3.8502	1.9251	0.5194
HNP−BH$\underline{H}_2$	−5.9408	−1.7562	4.1846	2.0923	0.4779
Ti(Etac-BH$\underline{H}_2$)			4.4742	2.2371	0.4470
Ti(Bzac-BH$\underline{H}_2$)	−5.4939	−2.4662	3.0277	1.5138	0.6605
Ti(Etac-SalH$\underline{H}_2$)	−5.0434	−1.7045	3.3389	1.6694	0.5990
Ti(Bzac-SalH$\underline{H}_2$)			2.9850	1.4925	0.6700
Ti(Etac-NH$\underline{H}_2$)	−4.9367	−3.1886	3.4352	1.7176	0.5822
Ti(Bzac-NH$\underline{H}_2$)			3.0032	1.5016	0.6660
Ti(HNP−NH$\underline{H}_2$)			2.9602	1.4801	0.6756
Ti(HNP−BH$\underline{H}_2$)	−4.9440	−3.3726	3.1267	1.5633	0.6396

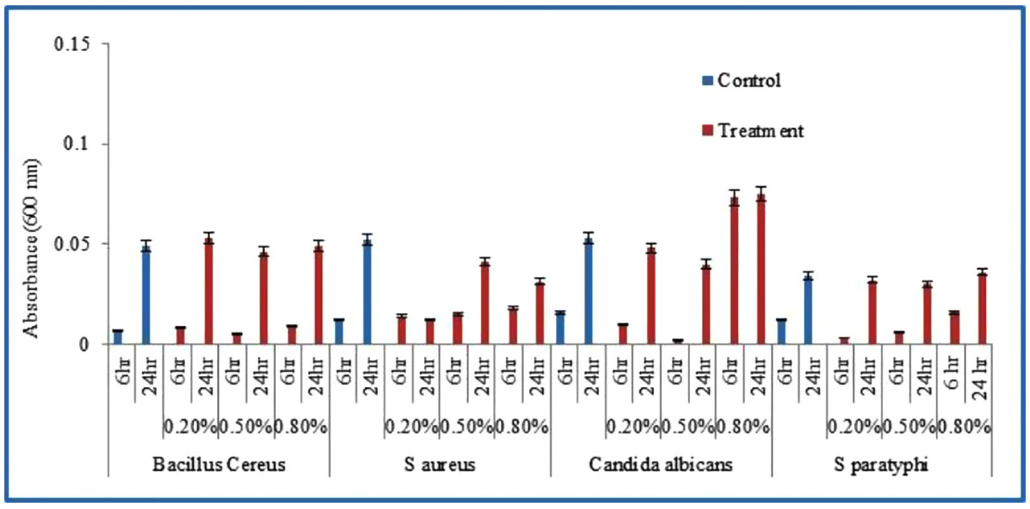

Fig. 8. Representative Presentation of bacterial activity of Etac-NH$\underline{H}_2$.

solutions against *Fusarium*. Fig. 9 shows the pH data of prepared ligands and complexes against *Fusarium* species. Figure shows that with the presence of fungal biomass showed higher pH (alkaline) after 3 days incubation. In the control *Fusarium* species became acidic (after 3 days), however in presence of test ligands and complexes the fungal medium became alkaline that means, pH of the sample S-1, S-2, S-3, S-4, S-6, S-7, S-8 became 7.96, 7.34, 6.92, 8.19, 7.32, 8.12, 6.24, 7.82 respectively. The Fig. 10 shows the fungal biomass result which was measured by dry weight measured technique. This figure showed that the test sample expressed more or less biomass after 3 days incubation. From the biomass of *Fusarium* species it is seen that S-1 and S-7 have the inducing capacity to enhance the aerial growth of this species whereas S-5 and S-6 have similar activity as the control. On the other hand S-2, S-3, S-4 and S-8 have the lower enhancing ability than the S-1 and S-7. The result indicated the test ligands and complexes have the tendency to increase microbial biomass of the *Fusarium* species.

3.8.2.2. Cup plate technique. The prepared ligands and complexes were also tested in vitro against fungi *Aspergillus niger* by cup plate technique. After incubation, the diameter of the zone of inhibition and zone of growth were measured in mm by a transparent scale. The ligand NH.Bzac$\underline{H}_2$ was showing growth inhibition activity against the tested fungi with respect to control. Rest of the ligands and the complexes were showing growth stimulation activity.

3.9. Antioxidant properties

3.9.1. Total phenolic content

In this investigation, TPC of Etac-NH$\underline{H}_2$, Ti(Etac-NH)$_2$, Bzac-HNP$\underline{H}_2$ and BH—HNPH$_2$ were 507.37 ± 1.227 mg/g dry weight, 271.08 ± 1.184 mg/g dry weight, 502 ± 3.287 mg/g dry weight and 416.48 ± 3.287 mg/g dry weight respectively. These test ligands and complex contain very high amount of phenolic content (Table 6) which means they have good antioxidant properties.

3.9.2. DPPH free radical scavenging activity

The DPPH assay is considered to be mainly based on an ET reaction, and hydrogen-atom abstraction is a marginal reaction pathway. DPPH is a source of free radical. So when a test sample is added in DPPH solution, the free radical is neutralized by the test sample which, either donate hydrogen or an electron which result

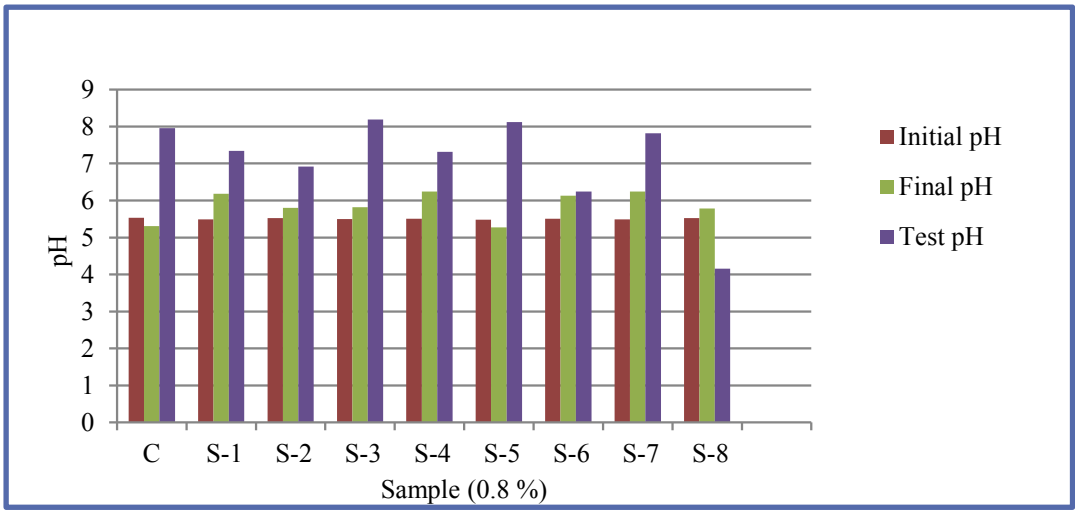

Fig. 9. pH data of prepared ligands and complexes against *Fusarium* species.

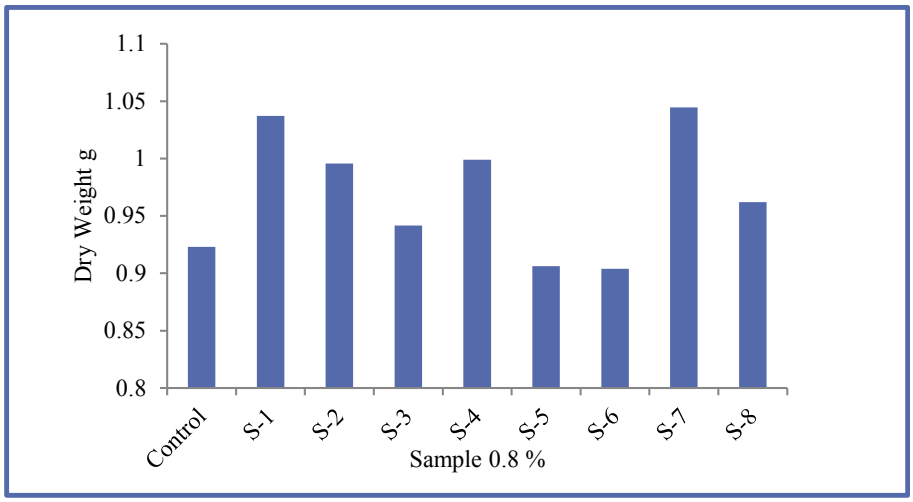

Fig. 10. Biomass of *Fusarium* species.

Table 6
Summary of the Total Phenolic Content estimation.

Sample	TPC (mg GAE/g dry weight)
Etac.$NH\underline{H}_2$	507.37 ± 1.227
Ti(Etac.$N\underline{H}$)$_2$	271.08 ± 1.184
Bzac.$NH\underline{H}_2$	502 ± 3.287
Ti(Bzac-$N\underline{H}$)$_2$	9.27 ± 0.279
HNP−$BH\underline{H}_2$	416.48 ± 3.287
Ti(HNP−$B\underline{H}$)$_2$	84.13 ± 1.812

in neutralization of free radical, and at 517 nm DPPH show absorbance due to this free radical. When the free radical is neutralized by test sample less free radical will be available. Due to this reason OD decreases and we calculate percentage of free radical neutralized/scavenged. Control should be greater than the sample, if its lower means, there is no inhibition takes place, instead of inhibit, it induces the activity. The absorbance of sample is higher than it might be due to the presence of colour compound or compound with their self-absorbance power. DPPH is stable nitrogen radical that bears no similarity to the highly reactive and transient peroxyl radicals involved in lipid peroxidation. Many antioxidants that react quickly with peroxyl radicals may react slowly or may even be inert to DPPH due to steric inaccessibility. In this experiment, the IC_{50} values of Etac-$NH\underline{H}_2$, Ti(Etac-NH)$_2$, NH-Bzac$\underline{H}_2$, BH−HNP$\underline{H}_2$ and standard ascorbic acid were found to be 5.74 μg/mL, 1.29 μg/mL, 1.32 μg/mL, 0.8 μg/mL and 1.34 μg/mL respectively. The values were anti-oxidative. The percentage of scavenging activity is very high as IC_{50} value is lower. Fig. 11 presents the comparison of DPPH free radical scavenging activity of selected ligands and their respective complexes with ascorbic acid (standard) in terms of IC_{50}.

4. Conclusion

From the IR spectra it is seen that, the bands observed between 1640 cm^{-1} and 1675 cm^{-1} for the free ligands were due to $\nu C=O$ and that obtained at 1600-1632 cm^{-1} were due to $\nu C=N$ of the azomethine group. The peak found for νTi-O at the range of 420–470 cm^{-1} indicating the complex formation. In the electronic spectral data, three main peaks were found for the ligands at

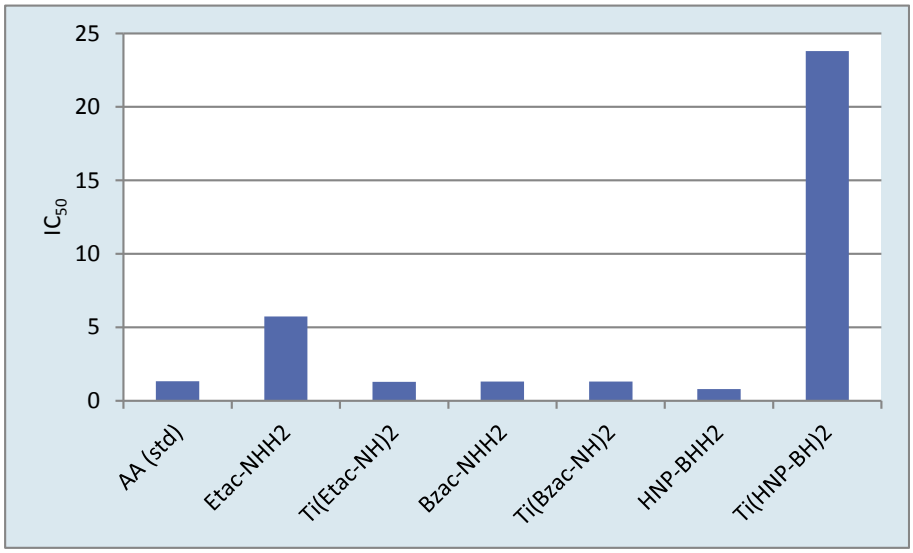

Fig. 11. Comparison of DPPH free radical scavenging activity of selected ligands and their respective complexes with ascorbic acid (standard) in terms of IC_{50}.

around 270, 320 and 370 nm. There was no evidence of any d-d transition, for the TiL_2 complexes, over the visible region. Absence of δ(−OH) peak in complexes and presence in ligands in the ^1H NMR spectra indicating the complex and ligand formation. Mass spectral evidence of the ligands and complexes showed relatively correct fragmentation pattern. All the prepared ligands in the enolic form have the potential to act as dinegative tridentate ligands in forming TiL_2 complexes. The computational study confirmed the octahedral geometry of the complexes. The test ligands and complexes have the inducing capacity to enhance the aerial growth of bacterial and fungal species. Antioxidant data indicated that Schiff base ligands have good antioxidant potential. They show more antioxidant properties than their Schiff base complexes.

References

[1] J.F. Lawrence, R.W. Frei, Chemical Derivatization in Chromatography, Elsevier, Amsterdam, 1976.
[2] H.A. El-Borae, J. Therm. Anal. Calorim. 81 (2005) 339.
[3] Z.M. Zaki, S.S. Haggag, A.A. Sayed, Spectrosc. Lett. 31 (2003) 757.
[4] L. Labib, L.A. Mohamed, M.F. Iskander, K. Griesar, W. Haase, Transition Met. Chem. 25 (2000) 700.
[5] A.O. Bulaov, B.S. Lukyanov, V.A. Kogan, V.V. Lukov, Russ. J. Coord. Chem. 28 (2002) 46.
[6] F. Al-Assar, K.N. Zelenin, E.E. Lesiovskaya, I.P. Bezhan, B.A. Chakchir, Pharm. Chem. J. 36 (2002) 598.
[7] V.K. Sharma, S. Srivastava, Synth. React. Inorg. Metal-Org. Nano-Metal Chem. 35 (2005) 311.
[8] O.V. Kotova, S.V. Eliseeva, A.S. Averjushkin, L.S. Lepnev, A.A. Vaschenko, A. Yu Rogachev, A. Vitukhnovskii, G. Kuzmina, Russ. Chem. Bull. 57 (2008) 1880.
[9] D.A. Chowdhury, M.N. Uddin, F. Hoque, CMU. J. Nat. Sci. 10 (2011) 261.
[10] S.M. Saadeh, Arab.J. Chem. 6 (2013) 191.
[11] M.N. Uddin, D.A. Chowdhury, M.K. Hossain, J. Chin. Chem. Soc. 59 (2012) 1520.
[12] D.A. Chowdhury, M.N. Uddin, M.A.H. Sarker, Chiang Mai J. Sci. 35 (2008) 483.
[13] M.P. Gleeson, D. Gleeson, J. Chem. Inf. Model. 49 (2009) 670.
[14] C. Lee, W. Yang, R.G. Parr, Phys. Rev. B 37 (1988) 785.
[15] A.D. Becke, Phys. Rev. A 38 (1988) 3098.
[16] M.J. Frisch, G.W. Trucks, H.B. Schlegel, G.E. Scuseria, M.A. Robb, J.R. Cheeseman, et al., Gaussian 09, Revision a. 02. Gaussian Inc, 2009. Wallingford, CT, Http//www. Gaussian. Com.
[17] R.G. Pearson, Proc. Natl. Acad. Sci. 83 (1986) 8440.
[18] I. Wiegand, K. Hilpert, R.E.W. Hancock, Nat. Protoc. 3 (2008) 163.
[19] M.N. Uddin, D.A. Chowdhury, M.T. Islam, F. Hoque, Orbital Electron. J. Chem. 4 (2012) 273.
[20] C. Johannes, S. Tuschy, I. Lamprecht, G. Obe, Biol. Zentralbl. 108 (1989) 15.
[21] C. Lin, C. Yu, S. Wu, K. Yih, J. Food Drug Anal. 17 (2009) 386.
[22] A.M. Hamil, K.M. Khalifa, A. Al-Houni, M.M. El-ajaily, Rasayan J. Chem. 2 (2009) 261.
[23] U.M. Rabie, A.S. Assran, M.H.M. Abou-El-Wafa, J. Mol. Struct. 872 (2008) 113.
[24] F.M. Morad, M.M. El-Sjaily, S.B. Gweirif, J. Sci. Appl. 1 (2007) 72.
[25] H. Yin, H. Xu, K. Li, G. Li, J. Inorg. Organomet. Polym. Mater. 15 (2005) 319.
[26] M. Tuncel, S. Serin, M. Tuncel, Trans. Met. Chem. 31 (2006) 805.
[27] N. Sharma, A.M. Thakur, S.S. Bhatt, S.C. Chaudhry, J. Chem. Sci. 119 (2007) 311.
[28] E.S. Meadows, S.L. De Wall, L.J. Barbour, J. Am. Chem. Soc. 122 (2000) 3325.
[29] J. Aihara, Theor. Chem. Acc.. 102(n.d.) 134.
[30] J. Aihara, J. Phys. Chem. A 103 (1999) 7487.